Impurity scattering effect on charge transport in high-T_c cuprate junctions

Y. Tanaka[1,2], Y. Asano[3], and S. Kashiwaya[4]

[1]*Department of Applied Physics, Nagoya University, Japan*
E-mail: ytanaka@nuap.nagoya-u.ac.jp

[2]*CREST, Japan Science and Technology Corporation, Japan*

[3]*Department of Applied Physics, Hokkaido University, Sapporo 060-8628, Japan*

[4]*NRI of AIST, Umezono, Tsukuba, Japan*

It is known that the zero-bias conductance peak (ZBCP) is expected in tunneling spectra of normal-metal / high-T_c cuprate junctions because of the formation of the midgap Andreev resonant states (MARS) at junction interfaces. In the present review, we report the recent theoretical study of impurity scattering effects on the tunneling spectroscopy. In the former part of the present paper, we discuss impurity effects in normal metal. We calculate tunneling conductance for diffusive normal metal (DN) / high T_c cuprate junctions based on the Keldysh Green's function technique. Besides the ZBCP due to the MARS, we can expect ZBCP caused by the different origin, i.e., the coherent Andreev reflection (CAR) assisted by the proximity effect in DN. Their relative importance depends on the angle α between the interface normal and the crystal axis of high-T_c superconductors. At $\alpha = 0$, we find the ZBCP by the CAR for low transparent junctions with small Thouless energies in DN; this is similar to the case of diffusive normal metal / insulator / s-wave superconductor junctions. Under increase of α from zero to $\pi/4$, the contribution of MARS to ZBCP becomes more prominent and the effect of the CAR is gradually suppressed. Such complex spectral features would be observable in conductance spectra of high-T_c junctions at very low temperatures. In the latter part of our paper, we study impurity effects in superconductors. We consider impurities near the junction interface on the superconductor side. The conductance is calculated from the Andreev and the normal reflection coefficients which are estimated by using the single-site approximation in an analytic calculation and by the recursive Green function method in a numerical simulation. We find splitting of the ZBCP in the presence of the time reversal symmetry. Thus the zero-field splitting of ZBCP in the experiment does not perfectly prove an existence of broken time reversal symmetry state.

PACS: 74.25.Fy, 74.25.Dw, 74.76.Bz

1. Introduction

Nowadays, charge transport in unconventional superconductor junctions has become one of the most important topics in solid state physics. The most remarkable property is the so-called zero bias conductance peak (ZBCP) observed in tunneling experiments. The ZBCP arises from the formation of midgap Andreev bound states (MARS) at the interface [1−5]. The MARS, which is created by injected and reflected quasiparticles feeling different signs of the pair poten-

tial, can play an important role in determining the pairing symmetry of unconventional superconductors. The experimental observation of the ZBCP has been reported for various unconventional superconductors of anisotropic pairing symmetries [5−20]. A basic theory of the ballistic transport in the presence of MARS has been formulated in Refs. 3,5. Stimulated by this theory, extensive studies of MARS in unconventional superconductor junctions have been performed during the last decade: in the case of broken time reversal symmetry state [21−28], in triplet superconductor

junctions [29−34], in quasi-one-dimensional organic superconductors [35−38], MARS and Doppler effect [39−43], MARS in ferromagnetic junctions [44−52], influence of MARS on Josephson effect [53−62], and other related problems [63−71]. However, the impurity scattering effect on the ZBCP in realistic normal metal/high-T_c cuprate junctions has not been clarified yet. The aim of present paper is to review the important progress in this issue.

The organization of the paper is as follows. In Sec. 2, we discuss the impurity scattering effect in normal metal. We calculate the tunneling conductance for diffusive normal metal (DN)/high-T_c cuprate junctions based on the Keldysh Green's function technique. Besides the ZBCP due to the MARS, we can expect ZBCP caused by a different mechanism, i.e., coherent Andreev reflection (CAR) assisted by proximity effect in DN. In Sec. 3, we discuss impurity effects in superconductors. The random potential near junction interfaces causes splitting of the ZBCP even in the presence of the time reversal symmetry.

2. Theory of charge transport in diffusive normal metal/high-T_c cuprate superconductor contacts

Before discussing charge transport in high-T_c cuprate junctions, we should review the progress of charge transport in mesoscopic superconducting systems. The low energy transport in mesoscopic superconducting systems is governed by Andreev reflection [72], a unique process specific to electron scattering at normal metal/superconductor interfaces. The phase coherence between incoming electrons and Andreev reflected holes persists at a mesoscopic length scale in the diffusive normal metal, which enhances interference effects on the probability of Andreev reflection [73]. The coherence plays an important role at sufficiently low temperatures and voltages when the energy broadening due to either voltages or temperatures becomes of the order of the Thouless energy E_{Th} in mesoscopic structures. As a result, the conductance spectra of mesoscopic junctions may be significantly modified by these interference effects. A remarkable experimental manifestation of the electron−hole phase coherence is the observation of the zero bias conductance peak (ZBCP) in diffusive normal metal (N)/superconductor (S) tunneling junctions [74−84].

Various theoretical models of charge transport in diffusive junctions extend the clean limit theories developed by Blonder, Tinkham and Klapwijk [85] (BTK) and Zaitsev [86]. In Refs. 87−92, the scattering matrix approach was used. On the other hand, the quasiclassical Green's function method in nonequilibrium superconductivity [93] is much more powerful

and convenient for the actual calculations of conductance for the arbitrary bias-voltages [94]. Using the Kuprianov and Lukichev (KL) boundary condition [95] for a diffusive SIN interface, Volkov, Zaitsev and Klapwijk (VZK) have obtained the conductance spectra with ZBCP, origin of which was attributed to coherent Andreev reflection (CAR) which induces the proximity effect in diffusive metal [94]. Several authors studied the charge transport in mesoscopic junctions combining this boundary condition with the Usadel [96] equation that describes superconducting correlations in diffusive metal [97−103]. The modified boundary conditions were studied by several authors [104,105]. Important progress was achieved by Nazarov [97,106] who developed a much more intuitive theory (the so-called «circuit theory») for matrix currents that allows to formulate boundary conditions for Usadel-like equations in the case of arbitrary transparencies [107]. Recently we have succeeded to extend this circuit theory for unconventional superconductors [108−110]. In order to resolve the charge transport in high-T_c cuprate junctions, we apply above theory for d-wave superconductors. We have shown that the formation of MARS strongly competes with the proximity effect that is an essential ingredient for CAR in diffusive conductor (DN). We consider a junction consisting of normal and superconducting reservoirs connected by a quasi-one-dimensional DN with a length L much larger than the elastic mean free path. The interface between the DN and the US (unconventional superconductor) electrode has a resistance R_b while the DN/N interface has zero resistance. The positions of the DN/N interface and the DN/S interface are denoted as $x = -L$ and $x = 0$, respectively. According to the circuit theory [106], the constriction area between DN and US is considered as composed of the diffusive isotropization zone, the left side ballistic zone, the right side ballistic zone and the scattering zone. The scattering zone is modeled as an insulating delta-function barrier with the transparency $T_n = 4\cos^2 \varphi/(4\cos^2 \varphi + Z^2)$, where Z is a dimensionless constant, φ is the injection angle measured from the interface normal to the junction and n is the channel index. We assume that the sizes of the ballistic and scattering zones along x axis is much shorter than the superconducting coherence length.

Here, we express insulating barrier as a delta-function model $H\delta(x)$, where Z is given by $Z = 2mH/(\hbar^2 k_F)$ with Fermi momentum k_F and effective mass m. In order to clarify charge transport in DN/US junctions, we must obtain Keldysh−Nambu Green's function, which has indices of transport channels and the direction of motion along x axis taking into account the proper boundary conditions. For this

purpose it is necessary to extend a general theory of boundary condition which covers the crossover from ballistic to diffusive cases [106] formulated for conventional junctions in the framework of the circuit theory [97,106]. However, the circuit theory cannot be directly applied to unconventional superconductors since it requires the isotropization. The latter is just incompatible with mere existence of unconventional superconductivity. To avoid this difficulty we restrict the discussion to a conventional model of *smooth interface* by assuming momentum conservation in the plane of the interface. We apply the quasiclassical Keldysh formalism for calculation of the conductance. The spatial dependence of 4×4 Green's function in DN $G_N(x)$ which is expressed in the matrix form as

$$\check{G}_N(x) = \begin{pmatrix} \hat{R}_N(x) & \hat{K}_N(x) \\ 0 & \hat{A}_N(x) \end{pmatrix}, \qquad (1)$$

should be determined. The Keldysh component $\hat{K}_N(x)$ is given by $\hat{K}_N(x) = \hat{R}_N(x)\hat{f}_1(x) - \hat{f}_1(x)\hat{A}_N(x)$ with retarded component $\hat{R}_N(x)$ and advanced component $\hat{A}_N(x)$ using distribution function $\hat{f}_1(x)$. We put the electrical potential zero in the S-electrode. In this case the spatial dependence of $\check{G}_N(x)$ in DN is determined by the static Usadel equation [96],

$$D \frac{\partial}{\partial x} \left[\check{G}_N(x) \frac{\partial \check{G}_N(x)}{\partial x} \right] + i \, [\check{H}, \check{G}_N(x)] = 0, \quad (2)$$

with the diffusion constant D in DN, where $\check{H}$ is given by

$$\check{H} = \begin{pmatrix} \hat{H}_0 & 0 \\ 0 & \hat{H}_0 \end{pmatrix} \qquad (3)$$

with $\hat{H}_0 = \varepsilon \hat{\tau}_3$.

The boundary condition for $\check{G}_N(x)$ at the DN/S interface is given by

$$\frac{L}{R_d} \left[\check{G}_N(x) \frac{\partial \check{G}_N(x)}{\partial x} \right] \Bigg|_{x=0_-} = -\frac{h}{2e^2 R_b} < \check{I} > . \quad (4)$$

$\check{I}$ is given by

$$\check{I} = \frac{2e^2}{h} \sum_n \check{I}_{n0}, \quad \check{I}_{n0} = 2 \, [\check{G}_1, \check{B}_n] \qquad (5)$$

with

$$\check{B}_n = (-T_{1n}[\check{G}_1, \check{H}_-^{-1}] + \check{H}_-^{-1}\check{H}_+ - T_{1n}^2 \check{G}_1 \check{H}_-^{-1}\check{H}_+ \check{G}_1)^{-1} \times$$
$$\times (T_{1n}(1 - \check{H}_-^{-1}) + T_{1n}^2 \check{G}_1 \check{H}_-^{-1}\check{H}_+). \qquad (7)$$

Here $\check{H}_\pm = (\check{G}_{2+} \pm \check{G}_{2-})/2$. R_d and R_b denote the resistance in DN and that at the DN/S interface, re-

spectively. The detailed derivation of the matrix current is shown in [109]. The average over the various angles of injected particles at the interface is defined as

$$\langle \, \check{I}(\varphi) \rangle = \int_{-\pi/2}^{\pi/2} d\varphi \cos\varphi \, \check{I}(\varphi) \, / \int_{-\pi/2}^{\pi/2} d\varphi T(\varphi) \cos\varphi \, , \, (8)$$

with $\check{I}(\varphi) = \check{I}$ and $T(\varphi) = T_n$. The resistance of the interface R_b is given by

$$R_b = \frac{h}{2e^2} \frac{2}{\displaystyle\int_{-\pi/2}^{\pi/2} d\varphi T(\varphi) \cos\varphi}. \qquad (9)$$

$\check{G}_N(-L)$ coincides with that in the normal state. We denote Keldysh−Nambu Green's function $\check{G}_1$, $\check{G}_{2\pm}$,

$$\check{G}_1 = \begin{pmatrix} \hat{R}_1 & \hat{K}_1 \\ 0 & \hat{A}_1 \end{pmatrix}, \quad \check{G}_{2\pm} = \begin{pmatrix} \hat{R}_{2\pm} & \hat{K}_{2\pm} \\ 0 & \hat{A}_{2\pm} \end{pmatrix}, \qquad (10)$$

where the Keldysh component $\hat{K}_{1,2\pm}$ is given by $\hat{K}_{1(2\pm)} = \hat{R}_{1(2\pm)}\hat{f}_{1(2)}(0) - \hat{f}_{1(2)}(0)\hat{A}_{1(2\pm)}$ with the retarded component $\hat{R}_{1,2\pm}$ and the advanced component $\hat{A}_{1,2\pm}$ using distribution function $\hat{f}_{1(2)}(0)$. In the above, $\hat{R}_{2\pm}$ is expressed by

$$\hat{R}_{2\pm} = (g_\pm \hat{\tau}_3 + f_\pm \hat{\tau}_2) \qquad (11)$$

with $g_\pm = \varepsilon/\sqrt{\varepsilon^2 - \Delta_\pm^2}$, $f_\pm = \Delta_\pm/\sqrt{\Delta_\pm^2 - \varepsilon^2}$, and $\hat{A}_{2\pm} = -\hat{\tau}_3 \hat{R}_{2\pm}^\dagger \hat{\tau}_3$ where ε denotes the quasiparticle energy measured from the Fermi energy. $\hat{f}_2(0) = = f_{0S}(0) = \tanh [\varepsilon/(2k_B T)]$ in thermal equilibrium with temperature T.

Using $\check{G}_N(x)$ one expresses the electric current as

$$I_{el} = \frac{-L}{4eR_d} \int_0^\infty d\varepsilon \, \mathrm{Tr} \left[\tau_3 \left(\check{G}_N(x) \frac{\partial \check{G}_N(x)}{\partial x} \right)^K \right] \quad (12)$$

where $\left(\check{G}_N(x) \dfrac{\partial \check{G}_N(x)}{\partial x} \right)^K$ denotes the Keldysh component of $\left(\check{G}_N(x) \dfrac{\partial \check{G}_N(x)}{\partial x} \right)$. In the actual calculation, we introduce a parameter $\theta(x)$ which is a measure of the proximity effect in DN where we denoted $\theta(0) = \theta_0$. Using $\theta(x)$, $\hat{R}_N(x)$ can be written as

$$\hat{R}_N(x) = \hat{\tau}_3 \cos\theta(x) + \hat{\tau}_2 \sin\theta(x). \qquad (13)$$

$\hat{A}_N(x)$ and $\hat{K}_N(x)$ satisfy the following equations: $\hat{A}_N(x) = -\tau_3 \hat{R}_N^\dagger(x)\hat{\tau}_3$, and $\hat{K}_N(x) = \hat{R}_N(x)\hat{f}_1(x) - \hat{f}_1(x)\hat{A}_N(x)$ with the distribution function

$\hat{f}_1(x)$ which is given by $\hat{f}_1(x) = f_{0N}(x) + \hat{\tau}_3 f_{3N}(x)$. In the above, $f_{3N}(x)$ is the relevant distribution function which determines the conductance of the junction we are now concentrating on. From the retarded or advanced component of the Usadel equation, the spatial dependence of $\theta(x)$ is determined by the following equation

$$D\frac{\partial^2}{\partial x^2}\theta(x) + 2i\varepsilon\sin[\theta(x)] = 0, \qquad (14)$$

while for the Keldysh component we obtain

$$D\frac{\partial}{\partial x}\left[\frac{\partial f_{3N}(x)}{\partial x}\cosh^2\theta_{\text{Im}}(x)\right] = 0 \qquad (15)$$

with $\theta_{\text{Im}}(x) = \text{Im}[\theta(x)]$. At $x = -L$, since DN is attached to the normal electrode, $\theta(-L) = 0$ and the condition $f_{3N}(-L) = f_{t0}$ is satisfied with

$$f_{t0} = \frac{1}{2}\left\{\tanh\left(\frac{\varepsilon + eV}{2k_BT}\right) - \tanh\left(\frac{\varepsilon - eV}{2k_BT}\right)\right\}, \quad (16)$$

where V is the applied bias voltage. Next, we focus on the boundary condition at the DN/S interface. Taking the retarded part of Eq. (4), we obtain

$$\frac{L}{R_d}\left.\frac{\partial\theta(x)}{\partial x}\right|_{x=0_-} = \frac{<F>}{R_b}, \qquad (17)$$

$$F = \frac{2T_n[\cos\theta_0(f_+ + f_-) - \sin\theta_0(g_+ + g_-)]}{(2 - T_n)(1 + g_+g_- + f_+f_-) + T_n[\cos\theta_0(g_+ + g_-) + \sin\theta_0(f_+ + f_-)]}. \qquad (18)$$

On the other hand, from the Keldysh part of Eq. (4), we obtain

$$\frac{L}{R_d}\left(\frac{\partial f_{3N}}{\partial x}\right)\cosh^2[\text{Im}(\theta_0)]\bigg|_{x=0_-} = -\frac{<I_{b0}> f_{3N}(0_-)}{R_b}, \qquad (19)$$

$$I_{b0} = \frac{T_n}{2}\frac{C_0 f_{3N}(0_-)}{|(2 - T_n)(1 + g_+g_- + f_+f_-) + T_n[\cos\theta_0(g_+ + g_-) + \sin\theta_0(f_+ + f_-)]|^2}, \qquad (20)$$

$$C_0 = T_n(1 + |\cos\theta_0|^2 + |\sin\theta_0|^2)[|g_+ + g_-|^2 + |f_+ + f_-|^2 + |1 + f_+f_- + g_+g_-|^2 + |f_+g_- - g_+f_-|^2] +$$

$$+ 2(2 - T_n)\text{Re}\{(1 + g_+^*g_-^* + f_+^*f_-^*)[(\cos\theta_0 + \cos\theta_0^*)(g_+ + g_-) + (\sin\theta_0 + \sin\theta_0^*)(f_+ + f_-)]\} +$$

$$+ 4T_n\text{Im}(\cos\theta_0\sin\theta_0^*)\text{Im}[(f_+ + f_-)(g_+^* + g_-^*)]. \qquad (21)$$

After a simple manipulation, we can obtain $f_{3N}(0_-)$

$$f_{3N}(0_-) = \frac{R_b f_{t0}}{R_b + \frac{R_d <I_{b0}>}{L}\displaystyle\int_{-L}^{0}\frac{dx}{\cosh^2\theta_{\text{Im}}(x)}}. \qquad (22)$$

Since the electric current I_{el} can be expressed via θ_0 in the form

$$I_{el} = -\frac{L}{eR_d}\int_0^\infty\left(\frac{\partial f_{3N}}{\partial x}\right)\bigg|_{x=0_-}\cosh^2[\text{Im}(\theta_0)]d\varepsilon, \quad (23)$$

we obtain the following final result for the current

$$I_{el} = \frac{1}{e}\int_0^\infty d\varepsilon\frac{f_{t0}}{\frac{R_b}{<I_{b0}>} + \frac{R_d}{L}\displaystyle\int_{-L}^{0}\frac{dx}{\cosh^2\theta_{\text{Im}}(x)}}. \qquad (24)$$

Then the total resistance R at zero temperature is given by

$$R = \frac{R_b}{<I_{b0}>} + \frac{R_d}{L}\int_{-L}^{0}\frac{dx}{\cosh^2\theta_{\text{Im}}(x)}. \qquad (25)$$

We will discuss the normalized conductance $\sigma_T(eV) = \sigma_S(eV)/\sigma_N(eV)$ where $\sigma_{S(N)}(eV)$ is the voltage-dependent conductance in the superconducting (normal) state given by $\sigma_S(eV) = 1/R$ and $\sigma_N(eV) = \sigma_N = 1/(R_d + R_b)$, respectively.

It should be remarked that in the present circuit theory, R_d/R_b can be varied independently of T_n, i.e., of Z, since we can change the magnitude of the constriction area independently. In the other words, R_d/R_b is no more proportional to $T_{av}(L/l)$, where T_{av} is the averaged transmissivity and l is the mean free path in the diffusive region, respectively. Based

on this fact, we can choose R_d/R_b and Z as independent parameters.

First, we focus on the line shapes of the conductance where *d*-wave symmetry is chosen as a pairing symmetry of unconventional superconductor. The pair potentials $\Delta_\pm$ are given by $\Delta_\pm = \Delta_0 \cos[2(\varphi \mp \alpha)]$ where α denotes the angle between the normal to the interface and the crystal axis of *d*-wave superconductors and Δ_0 is the maximum amplitude of the pair potential. In the above, φ denotes the injection angle of the quasiparticle measured from the *x* axis. It is known that quasiparticles with injection angle φ with $\pi/4 - |\alpha| < |\varphi| < \pi/4 + |\alpha|$ feel the MARS at the interface which induces ZBCP. In the following, we choose relatively strong barrier $Z = 10$. Results for high transparent cases are written in detail in Ref. 109.

Let us first choose $\alpha = 0$ where ZBCP due to the MARS is absent. We calculate $\sigma_T(eV)$ for various R_d/R_b. For $E_{Th} = \Delta_0$ [see Fig. 1,*a*], the magnitude of $\sigma_T(eV)$ for $|eV| < \Delta_0$ increases with the increase of R_d/R_b. First, the line shape of the voltage-dependent conductance remains to be *V* shaped and only the height of the bottom value is enhanced (curve *2* and *3*). The *V*-shaped line shape originates from the existence of nodes of the *d*-wave pair potential. Then, with a further increase of R_d/R_b, a rounded bottom structure (curve *4*) appears and finally it changes into a nearly flat line shape (curve *5*). For $E_{Th} = 0.01\Delta_0$ (Fig. 1,*b*), the magnitude of $\sigma_T(eV)$ has a ZBCP once the magnitude of R_d/R_b deviates slightly from 0. The order of the magnitude of the ZBCP width is given by E_{Th} as in the case of *s*-wave junctions [107]. When the magnitude of R_d/R_b exceeds unity, the $\sigma_T(eV)$ acquires a zero bias conductance dip (ZBCD) (curve *5*). The qualitative features of line shapes of $\sigma_T(eV)$ is different from those in *s*-wave junctions (see Figs. 1 and 2 in Ref. 37). It should be remarked that even in the case of *d*-wave junctions we can expect ZBCP by CAR as in the case of *s*-wave junction for $\alpha = 0$.

Next, we focus on $\sigma_T(eV)$ and θ_0 for $\alpha \neq 0$ $(0 < \alpha < \pi/4)$. First we focus on $\alpha = \pi/8$, where MARS is formed for $\pi/8 < |\varphi| < 3\pi/8$. $\sigma_T(eV)$ has a ZBCP due to the formation of MARS at the DN/US interface. The height of ZBCP is reduced with the increase of R_d/R_b (see Fig. 2,*a*). Contrary to the corresponding case of $\alpha = 0$, $\sigma_T(eV)$ is almost independent of E_{Th} (see Fig. 2,*b*). This is because proximity effect is almost suppressed due to the competition of MARS and the magnitude of $\theta(x)$ is reduced. In the extreme case, $\alpha = \pi/4$, the $\sigma_T(eV)$ is completely independent of E_{Th}. The obtained results is plotted in Fig. 3.

In the present Section, detailed theoretical investigation of the voltage-dependent conductance of diffu-
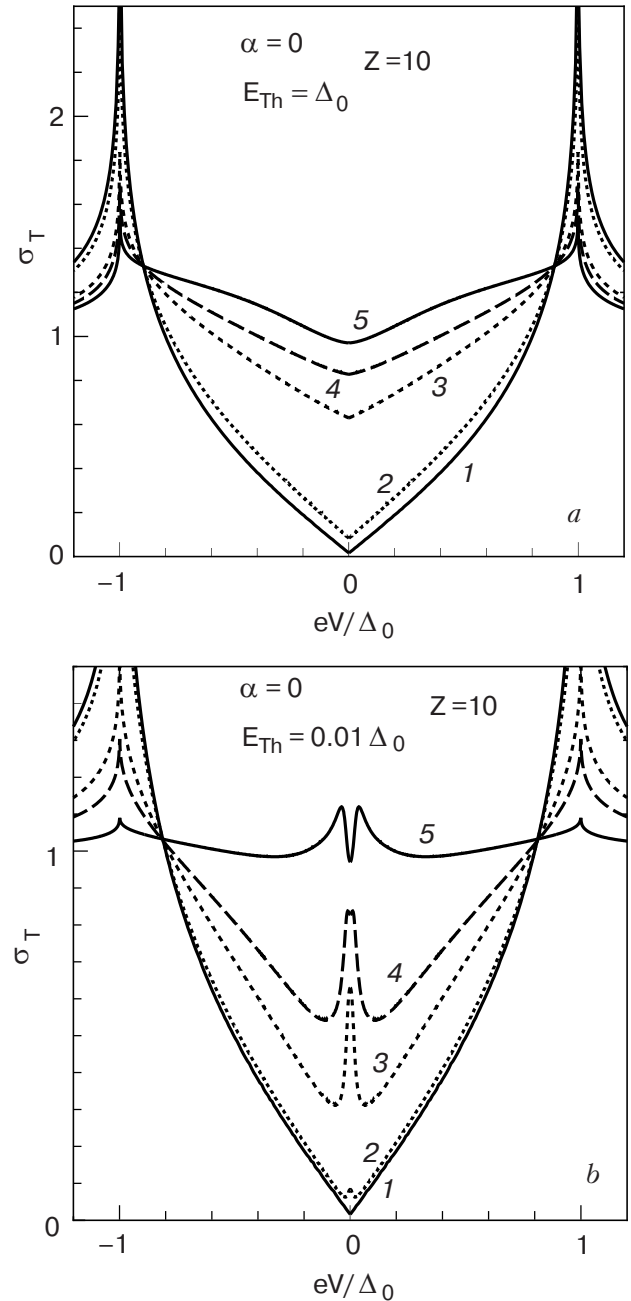

Fig. 1. Normalized conductance $\sigma_T(eV)$ for $Z = 10$, $\alpha = 0$, and $E_{Th} = \Delta_0$ (*a*), $E_{Th} = 0.01\Delta_0$ (*b*) at different R_d/R_b: 0 (*1*), 0.1 (*2*), 1 (*3*), 2 (*4*), and 10 (*5*).

sive normal metal/unconventional superconductor junctions is presented.

1. The ZBCP is frequently seen in the shape of $\sigma_T(eV)$. For $\alpha \neq 0$, the ZBCP is robust not depending on the diffusive resistance R_d. For $\alpha = 0$, ZBCP is due to the CAR.

2. The appearance of ZBCP is different for MARS and CAR mechanisms. The first mechanism may lead to arbitrary large $\sigma_T(0)$. The second mechanism cannot provide $\sigma_T(0)$ exceeding unity. While for the first mechanism the width of the ZBCP is determined by
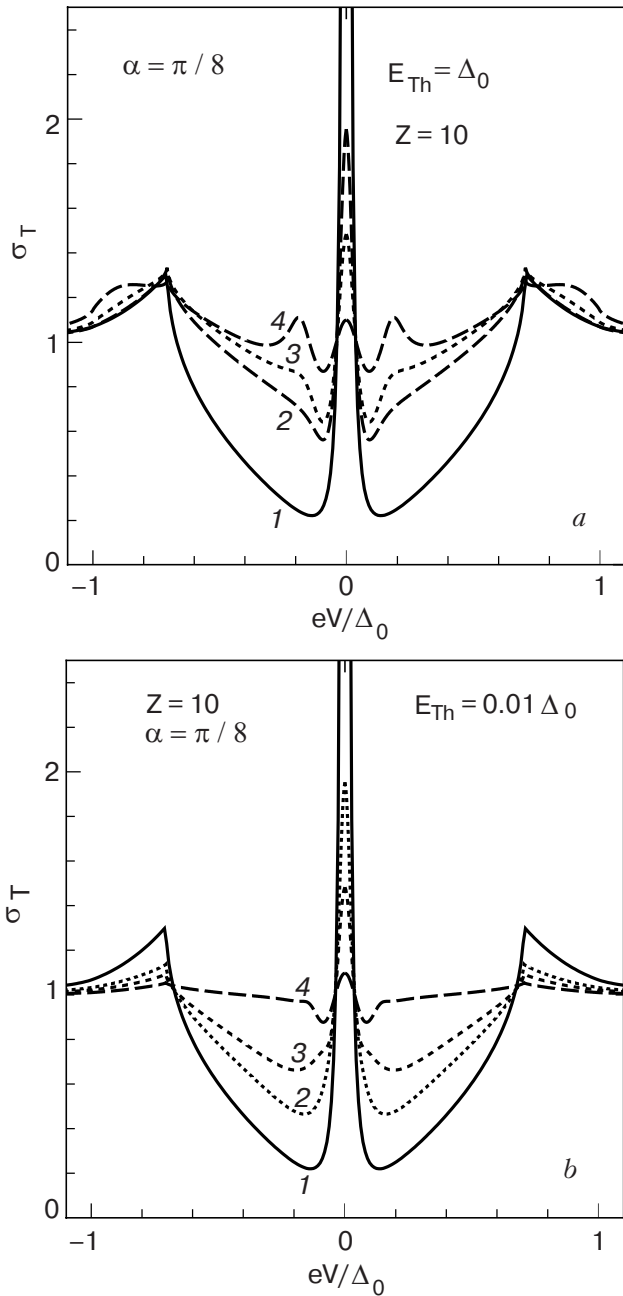
Fig. 2. Normalized conductance $\sigma_T(eV)$ for $\alpha = \pi/8$, $E_{Th} = \Delta_0$ (*a*) and $E_{Th} = 0.01\Delta_0$ (*b*) at different R_d/R_b: 0 (*1*), 1 (*2*), 2 (*3*), and 10 (*4*).

the transparency of the junction, it is determined by Thouless energy for the second one. These two mechanisms compete since the proximity effect and the MARS in singlet junctions are generally incompatible [108].

3. In the extreme case $\alpha = \pi/4$ the proximity effect and the CAR are absent. The $\sigma_T(eV)$ is then given by a simple Ohm's law: $\sigma_T(eV) = = (R_b + R_d)/(R_{R_d=0} + R_d)$; R_b being the resistance of the interface.

4. We have clarified various line shapes of the conductance including ZBCP. The obtained results serve
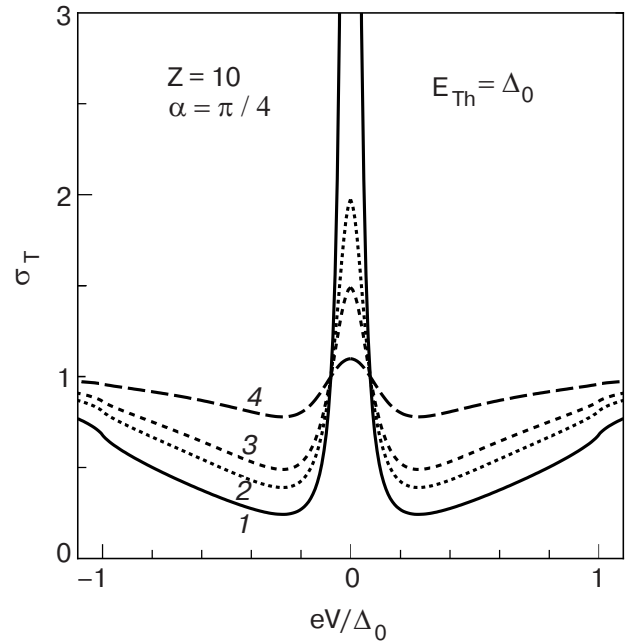

Fig. 3. Normalized conductance $\sigma_T(eV)$ for $\alpha = \pi/4$ at different R_d/R_b: 0 (*1*), 1 (*2*), 2 (*3*), and 10 (*4*).

as an important guide to analyze the actual experimental data of the tunneling spectra of high-T_c cuprate junctions. We want to stress that the height of ZBCP is strongly suppressed by the existence of DN and the resulting $\sigma_T(0)$ is not so high as obtained in the ballistic regime [3]. In the actual fit of the experimental data, we strongly hope to take into account the effect of R_d. In such a case without solving Usadel equation $\sigma_T(eV)$ can be simply approximated by

$$\sigma_T(eV) = \frac{R_d + R_b}{R_{R_d=0} + R_d}, \qquad (26)$$

$$R_{R_d=0} = \frac{R_b}{< I_{b0} >}, \qquad (27)$$

$$< I_{b0} > = \frac{\int_{-\pi/2}^{\pi/2} \cos\varphi \, I_{b0} \, d\varphi}{\int_{-\pi/2}^{\pi/2} \cos\varphi \, T(\varphi) \, d\varphi}, \qquad (28)$$

$$I_{b0} = \frac{T(\varphi)\{1 + T(\varphi)|\Gamma_+|^2 + [T(\varphi) - 1]|\Gamma_+\Gamma_-|^2\}}{|1 + [T(\varphi) - 1]\Gamma_+\Gamma_-|^2}, \qquad (29)$$

$$\Gamma_\pm = \frac{\Delta_\pm}{\varepsilon + \sqrt{\varepsilon^2 - \Delta_\pm^2}}, \qquad (30)$$

$$R_b = \frac{h}{2e^2} \frac{2}{\int_{-\pi/2}^{\pi/2} d\varphi \, T(\varphi) \cos\varphi}, \qquad (31)$$
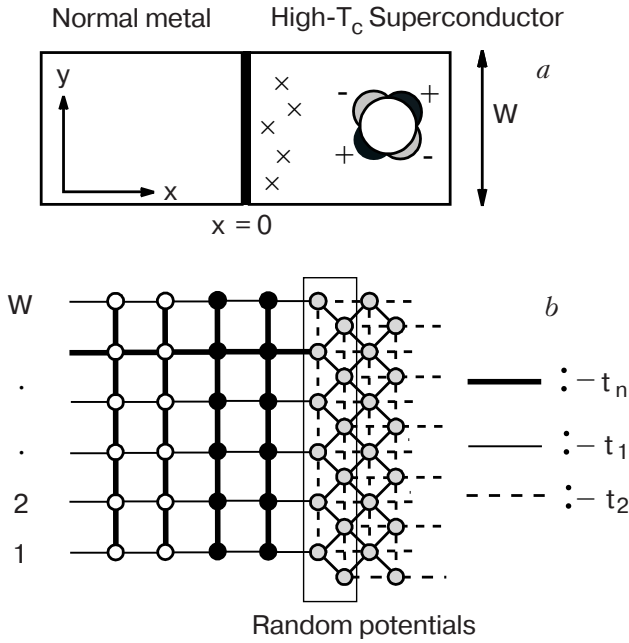
Fig. 4. The normal-metal / *d*-wave superconductor junction is schematically illustrated. In (*a*), crosses represent impurities. In (*b*), open, filled and gray circles represents the normal metal, insulator and superconductor, respectively.

with $\Delta_{\pm} = \Delta_0 \cos [2(\varphi \mp \alpha)]$ and $\varepsilon = eV$. This expression is a convenient one for the fit of the experimental data. However, for the quantitative discussions including much more general cases, one must solve Usadel equation as was done in the present paper. Recently, mesoscopic interference effects are observed in actual cuprate junctions [111]. We expect the present results will be observed in many experiments near future.

3. Impurity in high-T_c cuprate near the interface

The MARS is sensitive to the time reversal symmetry (TRS) of junctions because the retro-reflectivity of the Andreev reflection assists the constructive interference effect of a quasiparticle [112]. Actually, the ZBCP in NS junctions splits into two peaks under magnetic fields [25,39–43]. The peak splitting is also discussed [21–26,113,114] when the broken time reversal symmetry state (BTRSS) is formed at the interface. Theoretical studies showed that such BTRSS's are characterized by the $s + id_{xy}$ [26] or $d_{xy} + id_{x^2-y^2}$ [115] wave pairing symmetry. In the presence of the BTRSS, splitting of the ZBCP is expected in the zero magnetic field. Experimental results, however, are still controversial [116,117]. Some experiments re-

ported the split of the ZBCP at the zero magnetic field [9,17,18,118–122], other did not observe the splitting [8,10,11,15,20,123]. In addition, a recent experiment shows the almost absence of BTRSS in high-T_c grain boundary junctions [124].

In previous papers, we showed that random potentials at the NS interface cause the split of the ZBCP at the zero magnetic field by using the recursive Green function method in numerical simulations [55,125] and by the single-site approximation in an analytical calculation [126]. We also showed that the splitting due to the impurity scattering can be seen more clearly when realistic electronic structures of high-T_c materials are taken into account [127]. Our conclusion, however, contradicts to those of a number of theories [69–71,128,129] based on the quasiclassical Green function method [2,86,130–132]. The drastic suppression of the ZBCP by the interfacial randomness is the common conclusion of all the theories. The theories of the quasiclassical Green function method, however, concluded that the random potentials do not split the ZBCP. Thus this issue has not been fixed yet. There are mainly two reasons for the disagreement in the two theoretical approaches (i.e., the recursive Green function method and the quasiclassical Green function method). One is the treatment of the random potentials, the other is the effects of the rapidly oscillating wave functions on the conductance. In our simulations, we calculate the conductance without any approximation to the random potentials and the wave functions; this is an advantage of the recursive Green function method [55,133]. Our results indicate that the splitting of the ZBCP in experiments is not a direct evidence of the BTRSS at the interface of NS junctions.

Let us consider two-dimensional NS junctions as shown in Fig. 4,*a*, where normal metals ($x < 0$) and *d*-wave superconductors ($x > 0$) are separated by the potential barrier $V_B(\mathbf{r}) = H\delta(x)$. We assume the periodic boundary condition in the *y* direction and the width of the junction is W. The *a* axis of high-T_c superconductors is oriented by the 45 degrees from the interface normal. The pair potential of a high-T_c superconductor is described by $\Delta_{\mathbf{k}} = 2\Delta_0 \bar{k}_x \bar{k}_y$ in the momentum space, where $\bar{k}_x = k_x/k_F = \cos\varphi$ and $\bar{k}_y = k_y/k_F = \sin\varphi$ are the normalized wave number on the Fermi surface in the *x* and the *y* direction, respectively. The schematic figure of the pair potential is shown in Fig. 4. The NS junctions are described by the Bogoliubov−de Gennes equation,

$$\int d\mathbf{r}' \begin{pmatrix} \delta(\mathbf{r} - \mathbf{r}')h_0(\mathbf{r}') & \Delta(\mathbf{r}, \mathbf{r}') \\ \Delta^*(\mathbf{r}, \mathbf{r}') & -\delta(\mathbf{r} - \mathbf{r}')h_0(\mathbf{r}') \end{pmatrix} \begin{pmatrix} u(\mathbf{r}') \\ v(\mathbf{r}') \end{pmatrix} = E \begin{pmatrix} u(\mathbf{r}) \\ v(\mathbf{r}) \end{pmatrix}, \tag{32}$$

$$h_0(\mathbf{r}) = -\frac{\hbar^2 \nabla^2}{2m} + V(\mathbf{r}) - \mu_F, \qquad (33)$$

$$V(\mathbf{r}) = V_B(\mathbf{r}) + V_I(\mathbf{r}) \qquad (34)$$

where

$$\Delta(\mathbf{r}, \mathbf{r}') = \Theta(x)(1/V_{\text{vol}}) \sum_{\mathbf{k}} \Delta_{\mathbf{k}} \exp[i\mathbf{k}(\mathbf{r} - \mathbf{r}')].$$

The normal conductance of clean junctions is given by $G_N = (2e^2/h) N_c T_B$ with T_B being the transmission probability of the junction, $N_c = W k_F / \pi$ is the number of the propagating channels on the Fermi surface. In the low transparent junctions (i.e., $Z \gg 1$), we find $T_B \propto 1/Z^2$. In what follows, we redefine $z_0 = Z/2 = H m / \hbar^2 k_F$. We consider impurities near the interface on the superconductor side as indicated by crosses in Fig. 4. The potential of impurities is given by $V_I(\mathbf{r}) = V_i \sum_{j=1}^{N_i} \delta(\mathbf{r} - \mathbf{r}_j)$, where N_i is the number of impurities. Effects of impurities on the wave functions are taken into account by using the Lippmann–Schwinger equation,

$$\psi^{(l)}(\mathbf{r}) = \psi_0^{(l)}(\mathbf{r}) + \sum_{j=1}^{N_i} \hat{G}_0(\mathbf{r}, \mathbf{r}_j) V_i \hat{\sigma}_3 \psi^{(l)}(\mathbf{r}_j), \quad (35)$$

where l indicates a propagating channel characterized by the transverse wave number $k_y^{(l)}$ and $\hat{G}_0(\mathbf{r}, \mathbf{r}')$ are the real space Green functions in the clean junctions which can be obtained analytically. Here $\psi_0^{(l)}(\mathbf{r})$ is the wave function in which an electron like quasiparticle with $k_y^{(l)}$ is incident into the NS interface from normal metals and is described as

$$\psi_0^{(l)}(\mathbf{r}) = \chi_l(y) \left[\begin{pmatrix} 1 \\ 0 \end{pmatrix} \exp(ik_l x) + \right.$$

$$\left. + \begin{pmatrix} 0 \\ 1 \end{pmatrix} \exp(ik_l x) r_{NN}^{he}(l) + \begin{pmatrix} 1 \\ 0 \end{pmatrix} \exp(-ik_l x) r_{NN}^{ee}(l) \right],$$
$$(36)$$

for $x < 0$, where $\chi_l(y) = \exp[ik_y^{(l)} y]/\sqrt{W}$, k_l is the wave number of a quasiparticle in normal metals satisfying $k_l^2 + k_y^{(l)2} = k_F^2$, $r_{NN}^{ee}(l)$ and $r_{NN}^{he}(l)$ are the normal and the Andreev reflection coefficients of the clean junctions, respectively. The wave function for $x > 0$ is expressed in the same way. The wave function at an impurity $\psi^{(l)}(\mathbf{r}_{j'})$ can be obtained by $\mathbf{r} \to \mathbf{r}_{j'}$ in Eq. (35)

$$\psi_0^{(l)}(\mathbf{r}_{j'}) = \sum_{j=1}^{N_i} [\hat{\sigma}_0 \delta_{j,j'} - \hat{G}_0(\mathbf{r}_{j'}, \mathbf{r}_j) V_i \hat{\sigma}_3] \psi^{(l)}(\mathbf{r}_j).$$
$$(37)$$

It is possible to calculate the exact conductance if we obtain $\psi^{(l)}(\mathbf{r}_j)$ for all impurities by solving Eq. (37). In this paper, we solve Eq. (37) within the single-site approximation, where the multiple scattering effect involving many impurities (Anderson localization) are neglected. However the multiple scattering by an impurity is taken into account up to the infinite order of the scattering events. In the summation of j in Eq. (37), only the contribution with $j = j'$ is taken into account in the single-site approximation [134]. In this way, the wave function at $\mathbf{r}_j$ is approximately given by

$$\psi^{(l)}(\mathbf{r}_j) \approx [\hat{\sigma}_0 - \hat{G}_0(\mathbf{r}_j, \mathbf{r}_j) V_i \hat{\sigma}_3]^{-1} \psi_0^{(l)}(\mathbf{r}_j). \quad (38)$$

Substituting the wave function at impurities in Eq. (38) into Eq. (35), we obtain the wave function in the presence of impurities. The normal reflection coefficients $B_{l',l}$ and the Andreev reflection coefficients $A_{l',l}$ are then calculated analytically from the expression of the wave function for $x \to -\infty$. The differential conductance in NS junctions is calculated from the normal and the Andreev reflection coefficients [85],

$$G_{NS}(eV) = \frac{2e^2}{h} \int_{-\infty}^{\infty} dE \left(\frac{\partial f_{FD}(E - eV)}{\partial(eV)} \right) \times$$

$$\times \left[N_c g^{(0)} - 4 \sum_{j=1}^{N_i} \Gamma_j \right], \qquad (39)$$

$$g^{(0)} = 2 \int_0^{\pi/2} d\varphi \frac{\Delta_0^2 \cos^7 \varphi \sin^2 \varphi}{E^2 z_0^4 + \Delta_0^2 \cos^6 \varphi \sin^2 \varphi}. \quad (40)$$

The first term of Eq. (39), $N_c g^{(0)}$, is the conductance in clean junctions, $f_{FD}(E)$ is the Fermi–Dirac distribution function, and V is the bias-voltage applied to junctions. In Eq. (39), Γ_j represents effects of the impurity scattering on the conductance. Explicit expression of Γ_j is given in Ref. 126.

Before discussing the conductance, the local density of states (LDOS) near the junction interface should be clarified because LDOS affects the scattering events of a quasiparticle. The LDOS is given by

$$N_s(E, x) = -\frac{1}{\pi} \operatorname{Im} \operatorname{Tr} \hat{G}_0(\mathbf{r}, \mathbf{r}), \qquad (41)$$

$$= 4 N_0 z_0^2 \exp(-x/\xi_0) \times$$

$$\times \frac{2}{\pi} \int_0^{\pi/2} d\varphi \frac{\Delta_0^2 \cos^4 \varphi \sin^2 \varphi \sin^2(k_F x \cos \varphi)}{E^2 z_0^4 + \Delta_0^2 \cos^6 \varphi \sin^2 \varphi}. \quad (42)$$

In the second line, we use a condition $E \ll \Delta_0$ [126]. As shown in Fig. 5,*a*, the imaginary part of the Green function has a large peak around $E = 0$ reflecting the MARS formed at the junction interface, where $xk_F = 6$, $z_0 = 10$ and $\Delta_0 = 0.1\mu_F$. The energy scale $E_{ZEP} = \Delta_0/z_0^2$ characterizes the width of the peak of the LDOS. Since the self-energy of impurity scattering is roughly proportional to the LDOS, effects of scattering becomes strong for a quasiparticle with $E < E_{ZEP}$. At $E = 0$, we find

$$N_s(E = 0, x) \simeq 4N_0 z_0^2 \exp(-x/\xi_0)xk_F, \quad (43)$$

where $N_0 = m/(\pi\hbar^2)$ is the normal density of states in the unit area. In Fig. 5,*b*, we plot Eqs. (42) and (43) with the solid and broken lines, respectively. The results show the remarkable enhancement of the local density of states around $x \sim \xi_0$, where $\xi_0 = (\hbar v_F/\pi\Delta_0)$ is the coherence length and is about $6/k_F$. This implies that the MARS is formed around $x \sim \xi_0$.

In the presence of impurities, the self-energy of the impurity scattering depends on the LDOS. Thus the impurities around $x \sim \xi_0$ are expected to be strong scatterers. At the same time, scattering effects become remarkably strong around $E \sim 0$. The conductance in disordered junctions is shown in Fig. 6, where impurities are distributed randomly in the range of $1 < x_j k_F < L_s k_F$, $\rho_i = N_i \lambda_F^2/WL_s$ is the dimensionless area density of impurities and $z_0 = 10$. The conductance is calculated from the expression

$$G_{NS} = \frac{2e^2}{h} N_c \int_{-\infty}^{\infty} dE \left(\frac{\partial f_{FD}(E - eV)}{\partial(eV)} \right) \times$$

$$\times \left[g^{(0)} - \rho_i \frac{k_F L_s}{\pi} \langle \Gamma \rangle \right], \quad (44)$$

$$\langle \Gamma \rangle = \left\langle \frac{1}{N_i} \sum_{j=1}^{N_i} \Gamma_j \right\rangle, \quad (45)$$

where $\langle \cdots \rangle$ means the ensemble average. The broken line denotes the conductance in the clean limit. The width of the ZBCP in clean junctions is also characterized by E_{ZEP}. We choose $L_s k_F = 20$ in Fig. 6 because we focus on the impurities near the interface and $\xi_0 k_F \sim 6$. In Fig. 6,*a*, we show the conductance of junctions in which low density strong impurities are distributed (i.e., $V_i N_0 = 0.1$ and $\rho_i = 0.2$). The conductance for high density weak impurities (i.e., $V_i N_0 = 0.005$ and $\rho_i = 0.6$) is shown in Fig. 6,*b*. There is no peak splitting in Fig. 6,*a*, whereas the conductance clearly splits into two peaks in Fig. 6,*b* at the zero temperature. The impurity scattering affects the ZBCP in two ways: (i) it decreases the conductance around the zero-bias and (ii) it makes the ZBCP wider. Roughly speaking, the product of $V_i N_s(E = 0, \xi_0)$ characterizes the strength of the impurity scattering. The suppression of the zero-bias conductance always happens irrespective of $V_i N_s(E = 0, \xi_0)$. The widening, however, happens
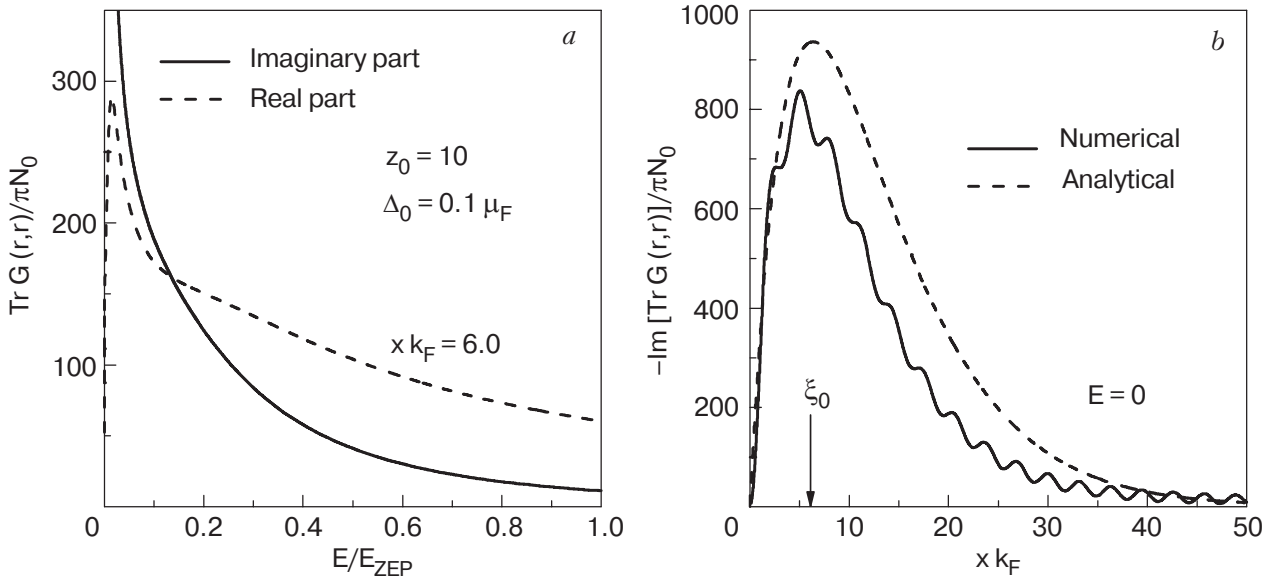

Fig. 5. In (*a*), the trace of the Green function in the superconductor is shown as a function of E. The peak width of the imaginary part is given by $E_{ZEP} = \Delta_0/z_0^2$. In (*b*), the local density of states is shown as a function of xk_F, where $E = 0$, $z_0 = 10$ and $\Delta_0 = 0.1\mu_F$. The numerical and analytical results are represented by the solid and broken lines, respectively.
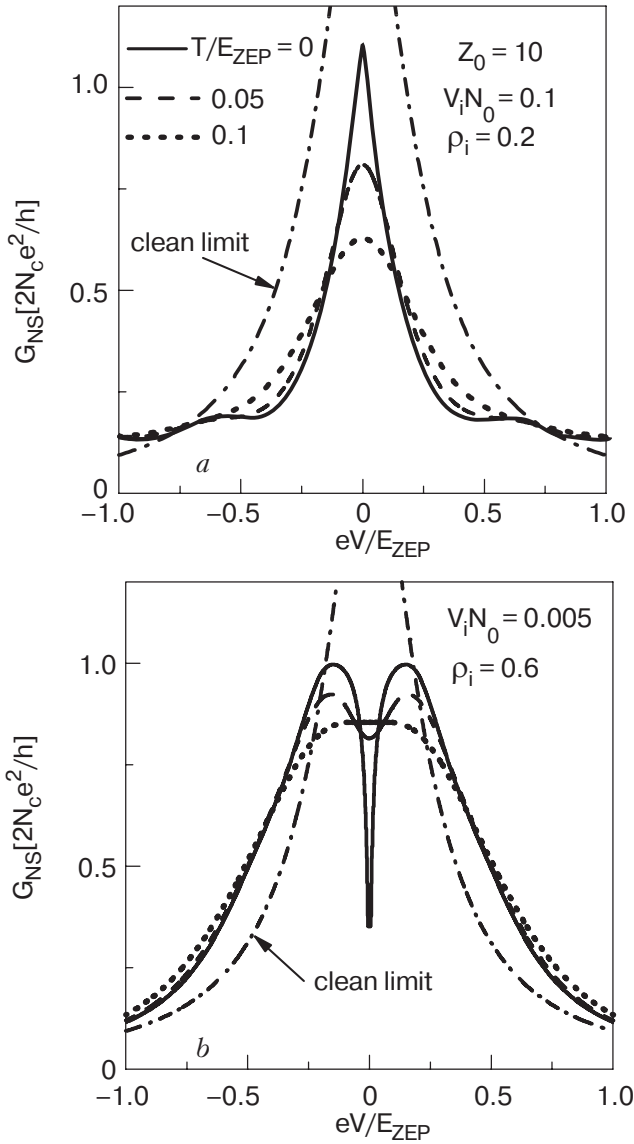
Fig. 6. The conductance in the presence of impurities distributed randomly in the range of $1 < x_j k_F < 20$, where ρ_i is the dimensionless area density of impurities near the interface. The conductance for low density strong impurities is shown in (*a*) with $V_i N_0 = 0.1$ and $\rho_i = 0.2$. The conductance for high density weak impurities with $V_i N_0 = 0.005$ and $\rho_i = 0.6$ are shown for several choices of temperatures (*b*). The conductance in the clean junction at the zero temperature is plotted with a dot-and-dash-line.

only if impurity scattering is sufficiently weak so that $V_i N_s (E = 0, \xi_0) \sim O(1)$ is satisfied [126]. Since $N_s (0, \xi_0)/N_0 \gg 1$ as shown in Fig. 6, the zero-bias conductance is drastically decreased by impurities. When $V_i N_s (0, \xi_0) \gg 1$ as shown in Fig. 6,*a*, the suppression of the zero-bias conductance dominates over the widening of the ZBCP. The conductance decreases from that in the clean junctions for almost the all bias region for $eV < E_{ZEP}$ as shown in Fig. 6,*a*, which leads to no splitting. On the other hand, for

weak scattering potentials, $V_i N_s (0, \xi_0) \sim O(1)$, impurities cause widening of the conductance peaks as well as the suppression of the zero-bias conductance. As a consequence, the conductance splits into two peaks as shown in Fig.6,*b*. The splitting peaks merge into a single peak under finite temperatures such as $T = 0.1 E_{ZEP}$ which is comparable to peak splitting width at the zero temperature. The results obtained indicate that the strong random potentials are not necessary for the split of the ZBCP. High density impurities with weak random potentials are responsible for the split of the ZBCP in low transparent junctions.

The analytical results can be confirmed by numerical simulations based on the recursive Green function method on two-dimensional tight-binding lattice as shown in Fig. 4,*b*. The system consists of three regions: a perfect normal metal (open circles), an insulator (filled circles) and a superconductor (gray circles). The gray sites correspond to Cu atoms on CuO_2 layers. The Hamiltonian reads,

$$\mathcal{H} = -\sum_{\mathbf{r},\mathbf{r}',\sigma}(t_{\mathbf{r},\mathbf{r}'}c^\dagger_{\mathbf{r},\sigma}c_{\mathbf{r}',\sigma} + \text{h.c.}) + \sum_{\mathbf{r},\sigma}(\varepsilon_\mathbf{r} - \mu)c^\dagger_{\mathbf{r},\sigma}c_{\mathbf{r},\sigma} -$$
$$-\sum_{\mathbf{r},\mathbf{r}'}(\Delta_{\mathbf{r}-\mathbf{r}'}c^\dagger_{\mathbf{r},\uparrow}c^\dagger_{\mathbf{r}',\downarrow} + \text{h.c.}) , \qquad (46)$$

where $t_{\mathbf{r},\mathbf{r}'}$ and $\Delta_{\mathbf{r}-\mathbf{r}'}$ are the hopping integral and the pair potential between $\mathbf{r}$ and $\mathbf{r}'$, respectively.

We consider the nearest neighbor hopping, t_n, in normal metals and insulators. The on-site potential $\varepsilon_\mathbf{r}$ is fixed at zero in normal metals and is V_B in insulators. In superconductors, we consider nearest neighbor hopping, t_1, and second nearest neighbor hopping, t_2. The random potential at the interface is taken into account through the on-site potential given randomly in a range of $-V_S/2 \leq \varepsilon_\mathbf{r} \leq V_S/2$ as shown in Fig. 4,*b*. The amplitude of the pair potential between the nearest neighbor sites is Δ_0 and the sign of the pair potential is determined to satisfy a *d*-wave symmetry. The Bogoliubov−de Gennes equation derived from the Hamiltonian of Eq. (46) is numerically solved by using the recursive Green function method [55]. The transmission and reflection coefficients of the junction are exactly computed in the simulation. We obtain the differential conductance from these coefficients based on the Blonder−Tinkham−Klapwijk formula [85].

In Fig. 7, we show the conductance as a function of the bias-voltage, where the Fermi energy in normal metals is $-2.0t_n$, $W = 30$ and the conductance is divided by the normal conductance of the junction G_N. The potential barrier at insulators is $V_B/t_n = 3.0$ and the transparency of insulating layers is of the order of 0.01. The Fermi energy μ_S, Δ_0, t_1, and t_2 are deter-
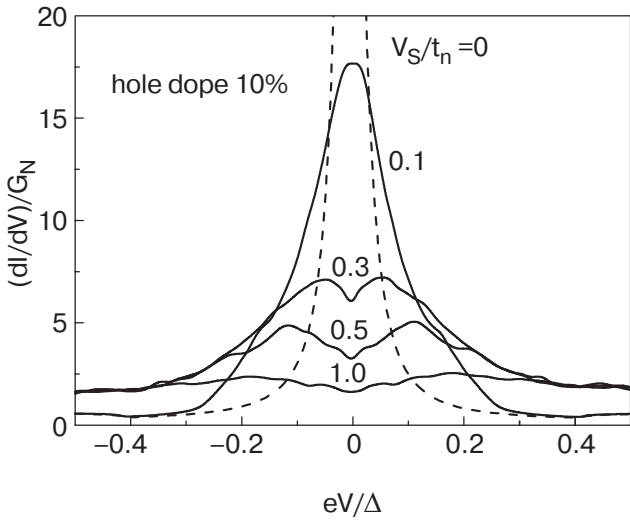
Fig. 7. The conductance calculated by the recursive Green function method. The degree of randomness is represented by V_S.

mined from an analysis of $t - J$ model [135] for 10% hole doping. The degree of disorder is $V_S/t_n = 0.0$ (broken lines), 0.1, 0.3, 0.5, and 1.0 from top to bottom. The conductance is averaged over a number of samples with different random configurations. The results show the drastic suppression of the ZBCP even for weak random potential at $V_S/t_n = 0.1$. The split of the ZBCP can be seen for slightly stronger potentials such as $V_S/t_n = 0.3$ and 0.5. For $V_S/t_n = 1.0$, we find dip structures around $eV \sim 0$ instead of the ZBCP. These results may correspond to the dip structures observed in disordered NS junctions in an experiment [136].

Several experiments [9,122] show a sensitivity of the conductance peaks to external magnetic fields. Here we discuss the conductance in the presence of magnetic fields. The effects of magnetic fields are taken into account phenomenologically by using the Aharonov−Bohm like phase shift [112,137] of a quasiparticle. Since the impurity scattering in magnetic
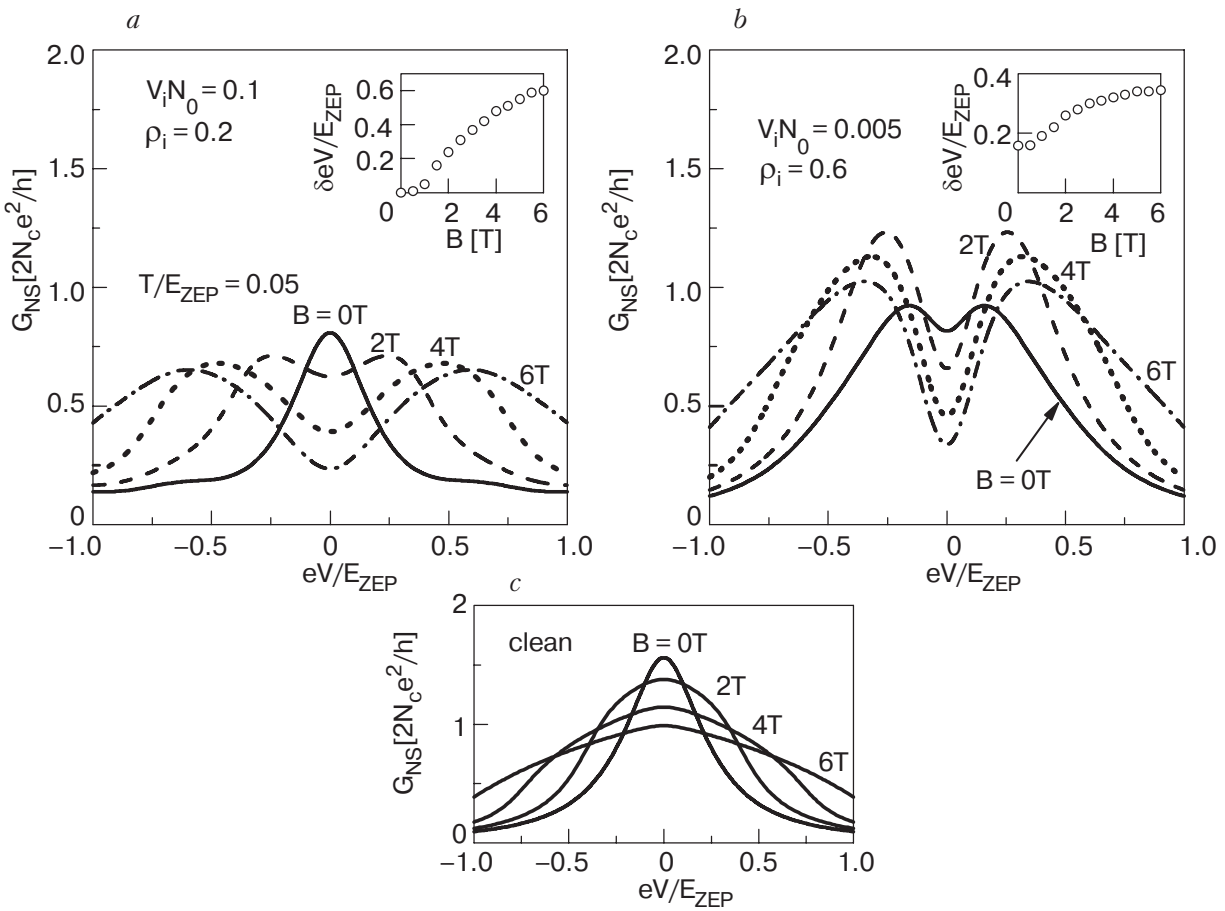

Fig. 8. The conductance under external magnetic fields for low density strong impurities with $V_i N_0 = 0.1$ and $\rho_i = 0.2$ are shown in (*a*), where T is fixed at $0.05 E_{ZEP}$. Those for high density weak impurities with $V_i N_0 = 0.005$ and $\rho_i = 0.6$ are shown in (*b*). In insets, peak positions are plotted as a function of magnetic fields. The conductance of clean junctions is shown in (*c*).

fields itself is a difficult problem to solve analytically, we neglect the interplay between magnetic fields and impurity scatterings. Within the phenomenological theory [112], effects of magnetic fields is considered by replacing E in Eq. (40) by $E + |\Delta_0 \cos\varphi \sin\varphi| \varphi_B$ as

$$g_B^{(0)} = \int_{-\pi/2}^{\pi/2} d\varphi \frac{\Delta_0^2 \cos^7\varphi \sin^2\varphi}{E_B^2 z_0^4 + \Delta_0^2 \cos^6\varphi \sin^2\varphi}, \quad (47)$$

$$E_B = E + 2\Delta_0 |\cos\varphi \sin\varphi| \varphi_B, \quad (48)$$

$$\varphi_B = 2\pi \frac{B\xi_0^2}{\varphi_0} \tan\varphi = B_0 \tan\varphi \quad (49)$$

where $\varphi_0 = 2\pi\hbar c/e$ and $B_0 = 0.001$ corresponds to $B = 1$ T. A quasiparticle acquires the Aharonov−Bohm like phase shift φ_B while moving near the NS interface [112]. In a previous paper, we found that ZBCP in clean junctions remains a single peak even in the strong magnetic fields [112] as shown in Fig. 8,*c*, where $z_0 = 10$ and $T = 0.05E_{\text{ZEP}}$. In Figs. 8,*a* and 8,*b*, we show the conductance in the presence of low density strong impurities and high density weak impurities, respectively, where V_i and ρ_i are same as those in Fig. 6,*a* and 6,*b*, respectively. A temperature is fixed at $T = 0.05E_{\text{ZEP}}$. In contrast to clean junctions in Fig. 8,*c*, the ZBCP in disordered junctions splits into two peaks under magnetic fields as shown in Fig. 8,*a*. The results obtained within the phenomenological theory indicate that the sensitivity of the ZBCP to magnetic fields depends on the degree of impurity scatterings. In insets, peak positions (δeV) are plotted with circles as a function of magnetic fields. For high density weak impurities in Fig. 8,*b*, we also found that the degree of peak splitting increases with increasing magnetic fields. In the limit of the strong fields, δeV tends to be saturated as shown in the inset. These characteristic behavior are found in the experiment [9].

In summary of this Section, we conclude that the impurity scattering causes the split of the ZBCP in normal-metal / high-T_c superconductor junctions. We consider impurities near the junction interface on the superconductor side. The conductance is calculated from the Andreev and the normal reflection coefficients which are estimated by using the single-site approximation in an analytic calculation and by the recursive Green function method in a numerical simulation. The strength of the impurity scattering depends on the transparency of the junction, the position of impurities and the energy of a quasiparticle because the MARS are formed at the interface. We find splitting of the ZBCP in the presence of the time reversal symmetry. Thus the zero-field splitting of

ZBCP in the experiment [9] does not perfectly prove an existence of BTRSS.

1. L.J. Buchholtz and G. Zwicknagl, *Phys. Rev.* **B23**, 5788 (1981); C.R. Hu, *Phys. Rev. Lett.* **72**, 1526 (1994).
2. C. Bruder, *Phys. Rev.* **B41**, 4017 (1990).
3. Y. Tanaka and S. Kashiwaya, *Phys. Rev. Lett.* **74**, 3451 (1995); S. Kashiwaya, Y. Tanaka, M. Koyanagi, and K. Kajimura, *Phys. Rev.* **B53**, 2667 (1996).
4. Y. Tanaka and S. Kashiwaya, *Phys. Rev.* **B53**, 9371 (1996).
5. S. Kashiwaya and Y. Tanaka, *Rep. Prog. Phys.* **63**, 1641 (2000) and references therein.
6. J. Geerk, X.X. Xi, and G. Linker, *Z. Phys.* **B73**, 329 (1988).
7. S. Kashiwaya, Y. Tanaka, M. Koyanagi, H. Takashima, and K. Kajimura, *Phys. Rev.* **B51**, 1350 (1995).
8. L. Alff, H. Takashima, S. Kashiwaya, N. Terada, H. Ihara, Y. Tanaka, M. Koyanagi, and K. Kajimura, *Phys. Rev.* **B55**, 14757 (1997).
9. M. Covington, M. Aprili, E. Paraoanu, L.H. Greene, F. Xu, J. Zhu, and C.A. Mirkin, *Phys. Rev. Lett.* **79**, 277 (1997).
10. J.Y.T. Wei, N.-C. Yeh, D.F. Garrigus, and M. Strasik, *Phys. Rev. Lett.* **81**, 2542 (1998).
11. I. Iguchi, W. Wang, M. Yamazaki, Y. Tanaka, and S. Kashiwaya, *Phys. Rev.* **B62**, R6131 (2000).
12. F. Laube, G. Goll, H.v. Löhneysen, M. Fogelström, and F. Lichtenberg, *Phys. Rev. Lett.* **84**, 1595 (2000).
13. Z.Q. Mao, K.D. Nelson, R. Jin, Y. Liu, and Y. Maeno, *Phys. Rev. Lett.* **87**, 037003 (2001).
14. Ch. Wälti, H.R. Ott, Z. Fisk, and J.L. Smith, *Phys. Rev. Lett.* **84**, 5616 (2000).
15. H. Aubin, L.H. Greene, Sha Jian, and D.G. Hinks, *Phys. Rev. Lett.* **89**, 177001 (2002).
16. Z.Q. Mao, M.M. Rosario, K.D. Nelson, K. Wu, I.G. Deac, P. Schiffer, Y. Liu, T. He, K.A. Regan, and R.J. Cava, *Phys. Rev.* **B67**, 094502 (2003).
17. A. Sharoni, O. Millo, A. Kohen, Y. Dagan, R. Beck, G. Deutscher, and G. Koren, *Phys. Rev.* **B65**, 134526 (2002).
18. A. Kohen, G. Leibovitch, and G. Deutscher, *Phys. Rev. Lett.* **90**, 207005 (2003).
19. M.M. Qazilbash, A. Biswas, Y. Dagan, R.A. Ott, and R.L. Greene, *Phys. Rev.* **B68**, 024502 (2003).
20. J.W. Ekin, Y. Xu, S. Mao, T. Venkatesan, D.W. Face, M. Eddy, and S.A. Wolf, *Phys. Rev.* **B56**, 13746 (1997).
21. Y. Tanuma, Y. Tanaka, M. Yamashiro, and S. Kashiwaya, *Phys. Rev.* **B57**, 7997 (1998).
22. Y. Tanuma, Y. Tanaka, M. Ogata, and S. Kashiwaya, *J. Phys. Soc. Jpn.* **67**, 1118 (1998).
23. Y. Tanuma, Y. Tanaka, M. Ogata, and S. Kashiwaya, *Phys. Rev.* **B60**, 9817 (1999).
24. Y. Tanuma, Y. Tanaka, and S. Kashiwaya, *Phys. Rev.* **B64**, 214519 (2001).
25. M. Fogelström, D. Rainer, and J.A. Sauls, *Phys. Rev. Lett.* **79**, 281 (1997); D. Rainer, H. Burkhardt, M. Fo-

gelström, and J.A. Sauls, *J. Phys. Chem. Solids* **59**, 2040 (1998).

26. M. Matsumoto and H. Shiba, *J. Phys. Soc. Jpn.* **64**, 1703 (1995); M. Matsumoto and H. Shiba, *J. Phys. Soc. Jpn.* **64**, 4867 (1995).

27. L.J. Buchholtz, M. Palumbo, D. Rainer, and J.A. Sauls, *J. Low Temp. Phys.* **101**, 1097 (1995).

28. Y. Tanaka and S. Kashiwaya, *Phys. Rev.* **B58**, 2948 (1998).

29. M. Yamashiro, Y. Tanaka, and S. Kashiwaya, *Phys. Rev.* **B56**, 7847 (1997).

30. M. Yamashiro, Y. Tanaka, Y. Tanuma, and S. Kashiwaya, *J. Phys. Soc. Jpn.* **67**, 3224 (1998).

31. M. Yamashiro, Y. Tanaka, and S. Kashiwaya, *J. Phys. Soc. Jpn.* **67**, 3364 (1998).

32. M. Yamashiro, Y. Tanaka, Y. Tanuma, and S. Kashiwaya, *J. Phys. Soc. Jpn.* **68**, 2019 (1999).

33. C. Honerkamp and M. Sigrist, *Prog. Theor. Phys.* **100**, 53 (1998).

34. Y. Asano, Y. Tanaka, Y. Matsuda, and S. Kashiwaya, *Phys. Rev.* **B68**, 184506 (2003).

35. Y. Tanuma, K. Kuroki, Y. Tanaka, and S. Kashiwaya, *Phys. Rev.* **B64**, 214510 (2001).

36. K. Sengupta, I. utiæ, H.-J. Kwon, V.M. Yakovenko, and S. Das Sarma, *Phys. Rev.* **B63**, 144531 (2001).

37. Y. Tanuma, K. Kuroki, Y. Tanaka, R. Arita, S. Kashiwaya, and H. Aoki, *Phys. Rev.* **B66**, 094507 (2002).

38. Y. Tanuma, K. Kuroki, Y. Tanaka, and S. Kashiwaya, *Phys. Rev.* **B68**, 214513 (2003)

39. Y. Tanuma, Y. Tanaka, K. Kuroki, and S. Kashiwaya, *Phys. Rev.* **B66**, 174502 (2002).

40. Y. Tanaka, H. Tsuchiura, Y. Tanuma, and S. Kashiwaya, *J. Phys. Soc. Jpn.* **71**, 271 (2002).

41. Y. Tanaka, Y. Tanuma, K. Kuroki, and S. Kashiwaya, *J. Phys. Soc. Jpn.* **71**, 2102 (2002).

42. Y. Tanaka, H. Itoh, H. Tsuchiura, Y. Tanuma, J. Inoue, and S. Kashiwaya, *J. Phys. Soc. Jpn.* **71**, 2005 (2002).

43. Yu.S. Barash, M.S. Kalenkov, and J. Kurkijarvi, *Phys. Rev.* **B62**, 6665 (2000).

44. J.-X. Zhu, B. Friedman, and C.S. Ting, *Phys. Rev.* **B59**, 9558 (1999).

45. S. Kashiwaya, Y. Tanaka, N. Yoshida, and M.R. Beasley, *Phys. Rev.* **B60**, 3572 (1999).

46. I. Zutic and O.T. Valls, *Phys. Rev.* **B60**, 6320 (1999).

47. N. Yoshida, Y. Tanaka, J. Inoue, and S. Kashiwaya, *J. Phys. Soc. Jpn.* **68**, 1071 (1999).

48. T. Hirai, N. Yoshida, Y. Tanaka, J. Inoue, and S. Kashiwaya, *J. Phys. Soc. Jpn.* **70**, 1885 (2001).

49. N. Yoshida, H. Itoh, T. Hirai, Y. Tanaka, J. Inoue, and S. Kashiwaya, *Physica* **C367**, 135 (2002).

50. T. Hirai, Y. Tanaka, N. Yoshida, Y. Asano, J. Inoue, and S. Kashiwaya, *Phys. Rev.* **B67**, 174501 (2003).

51. Y. Tanaka and S. Kashiwaya, *J. Phys. Soc. Jpn.* **68**, 3485 (1999).

52. Y. Tanaka and S. Kashiwaya, *J. Phys. Soc. Jpn.* **69**, 1152 (2000).

53. Y. Tanaka and S. Kashiwaya, *Phys. Rev.* **B53**, 11957 (1996); Y. Tanaka and S. Kashiwaya, *Phys. Rev.* **B56**, 892 (1997).

54. E. Il'ichev, V. Zakosarenko, R.P.J. IJsselsteijn, V. Schultze, H.-G. Meyer, H.E. Hoenig, H. Hilgenkamp, and J. Mannhart, *Phys. Rev. Lett.* **81**, 894 (1998).

55. Y. Asano, *Phys. Rev.* **B63**, 052512 (2001).

56. Y. Asano, *Phys. Rev.* **B64**, 014511 (2001).

57. Y. Asano, *Phys. Rev.* **B64**, 224515 (2001).

58. Y. Asano, *J. Phys. Soc. Jpn.* **71**, 905 (2002).

59. Y. Asano, Y. Tanaka, M. Sigrist, and S. Kashiwaya, *Phys. Rev.* **B67**, 184505 (2003).

60. Y.S. Barash, H. Burkhardt, and D. Rainer, *Phys. Rev. Lett.* **77**, 4070 (1996).

61. E. Ilichev, M. Grajcar, R. Hlubina, R.P.J. IJsselsteijn, H.E. Hoenig, H.-G. Meyer, A. Golubov, M.H.S. Amin, A.M. Zagoskin, A.N. Omelyanchouk, and M.Yu. Kuprianov, *Phys. Rev. Lett.* **86**, 5369 (2001).

62. G. Testa, A. Monaco, E. Esposito, E. Sarnelli, D.-J. Kang, E.J. Tarte, S.H. Mennema, and M.G. Blamire, *cond-mat/0310727*.

63. Y. Tanaka, T. Hirai, K. Kusakabe, and S. Kashiwaya, *Phys. Rev.* **B60**, 6308 (1999).

64. T. Hirai, K. Kusakabe, and Y. Tanaka, *Physica* **C336**, 107 (2000); K. Kusakabe, and Y. Tanaka, *Physica* **C367**, 123 (2002); K. Kusakabe and Y. Tanaka, *J. Phys. Chem. Solids* **63**, 1511 (2002).

65. N. Stefanakis, *Phys. Rev.* **B64**, 224502 (2001).

66. Z.C. Dong, D.Y. Xing, and Jinming Dong, *Phys. Rev.* **B65**, 214512 (2002); Z.C. Dong, D.Y. Xing, Z.D. Wang, Ziming Zheng, and Jinming Dong, *Phys. Rev.* **B63**, 144520 (2001).

67. M.H.S. Amin, A.N. Omelyanchouk, and A.M. Zagoskin, *Phys. Rev.* **B63**, 212502 (2001).

68. Shin-Tza Wu and Chung-Yu Mou, *Phys. Rev.* **B66**, 012512 (2002).

69. A.A. Golubov and M.Y. Kuprianov, *Pis'ma Zh. Eksp. Teor. Fiz* **69**, 242 (1999)[*Sov. Phys. JETP Lett.* **69**, 262 (1999)]; *ibid.* **67**, 478 (1998)[*Sov. Phys. JETP Lett.* **67**, 501 (1998)].

70. A. Poenicke, Yu.S. Barash, C. Bruder, and V. Istyukov, *Phys. Rev.* **B59**, 7102 (1999); K. Yamada, Y. Nagato, S. Higashitani, and K. Nagai, *J. Phys. Soc. Jpn.* **65**, 1540 (1996).

71. T. Lück, U. Eckern, and A. Shelankov, *Phys. Rev.* **B63**, 064510 (2002) .

72. A.F. Andreev, *Sov. Phys. JETP* **19**, 1228 (1964).

73. F.W.J. Hekking and Yu.V. Nazarov, *Phys. Rev. Lett.* **71**, 1625 (1993).

74. F. Giazotto, P. Pingue, F. Beltram, M. Lazzarino, D. Orani, S. Rubini, and A. Franciosi, *Phys. Rev. Lett.* **87**, 216808 (2001).

75. T.M. Klapwijk, *Physica* **B197**, 481 (1994).

76. A. Kastalsky, A.W. Kleinsasser, L.H. Greene, R. Bhat, F.P. Milliken, and J.P. Harbison, *Phys. Rev. Lett.* **67**, 3026 (1991).

77. C. Nguyen, H. Kroemer, and E.L. Hu, *Phys. Rev. Lett.* **69**, 2847 (1992).

78. B.J. van Wees, P. de Vries, P. Magnee, and T.M. Klapwijk, *Phys. Rev. Lett.* **69**, 510 (1992).

79. J. Nitta, T. Akazaki, and H. Takayanagi, *Phys. Rev.* **B49**, 3659 (1994).

80. S.J.M. Bakker, E. van der Drift, T.M. Klapwijk, H.M. Jaeger, and S. Radelaar, *Phys. Rev.* **B49**, 13275 (1994).

81. P. Xiong, G. Xiao, and R.B. Laibowitz, *Phys. Rev. Lett.* **71**, 1907 (1993).

82. P.H.C. Magnee, N. van der Post, P.H.M. Kooistra, B.J. van Wees, and T.M. Klapwijk, *Phys. Rev.* **B50**, 4594 (1994).

83. J. Kutchinsky, R. Taboryski, T. Clausen, C.B. Sorensen, A. Kristensen, P.E. Lindelof, J. Bindslev Hansen, C. Schelde Jacobsen, and J.L. Skov, *Phys. Rev. Lett.* **78**, 931 (1997).

84. W. Poirier, D. Mailly, and M. Sanquer, *Phys. Rev. Lett.* **79**, 2105 (1997).

85. G.E. Blonder, M. Tinkham, and T.M. Klapwijk, *Phys. Rev.* **B25**, 4515 (1982).

86. A.V. Zaitsev, *Zh. Eksp. Teor. Fiz.* **86**, 1742 (1984) [*Sov. Phys. JETP* **59**, 1015 (1984)].

87. C.W.J. Beenakker, *Rev. Mod. Phys.* **69**, 731 (1997).

88. C.J. Lambert, *J. Phys. Cond. Matter* **3**, 6579 (1991).

89. Y. Takane and H. Ebisawa, *J. Phys. Soc. Jpn.* **61**, 2858 (1992).

90. C.W.J. Beenakker, *Phys. Rev.* **B46**, 12841 (1992).

91. C.W.J. Beenakker, B. Rejaei, and J.A. Melsen, *Phys. Rev. Lett.* **72**, 2470 (1994).

92. G.B. Lesovik, A.L. Fauchere, and G. Blatter, *Phys. Rev.* **B55**, 3146 (1997).

93. A.I. Larkin and Yu.V. Ovchinnikov, *Sov. Phys. JETP* **41**, 960 (1975).

94. A.F. Volkov, A.V. Zaitsev, and T.M. Klapwijk, *Physica* **C210**, 21 (1993).

95. M.Yu. Kuprianov and V.F. Lukichev, *Zh. Exp. Teor. Fiz.* **94**, 139 (1988) [*Sov. Phys. JETP* **67**, 1163 (1988)].

96. K.D. Usadel, *Phys. Rev. Lett.* **25**, 507 (1970).

97. Yu.V. Nazarov, *Phys. Rev. Lett.* **73**, 1420 (1994).

98. S. Yip, *Phys. Rev.* **B52**, 3087 (1995).

99. Yu.V. Nazarov and T.H. Stoof, *Phys. Rev. Lett.* **76**, 823 (1996); T.H. Stoof and Yu.V. Nazarov, *Phys. Rev.* **B53**, 14496 (1996).

100. A.F. Volkov, N. Allsopp, and C.J. Lambert, *J. Phys. Cond. Matter.* **8**, L45 (1996); A.F. Volkov and H. Takayanagi, *Phys. Rev.* **B56**, 11184 (1997).

101. A.A. Golubov, F.K. Wilhelm, and A.D. Zaikin, *Phys. Rev.* **B55**, 1123 (1997).

102. R. Seviour and A.F. Volkov, *Phys. Rev.* **B61**, R9273 (2000).

103. W. Belzig, F.K. Wilhelm, C. Bruder, et al., *Superlatt. Microstruct.* **25**, 1251 (1999).

104. C.J. Lambert, R. Raimondi, V. Sweeney, and A.F. Volkov, *Phys. Rev.* **B55**, 6015 (1997).

105. E.V. Bezuglyi, E.N. Bratus', V.S. Shumeiko, G. Wendin, and H. Takayanagi, *Phys. Rev.* **B62**, 14439 (2000).

106. Yu.V. Nazarov, *Superlatt. Microstruct.* **25** 1221 (1999), *cond-mat/9811155*.

107. Y. Tanaka, A.A. Golubov, and S. Kashiwaya, *Phys. Rev.* **B68**, 054513 (2003).

108. Y. Tanaka, Y.V. Nazarov, and S. Kashiwaya, *Phys. Rev. Lett.* **90**, 167003 (2003).

109. Y. Tanaka, Y.V. Nazarov, A. Golubov, and S. Kashiwaya, *Phys. Rev.* **B69**, 144519 (2004).

110. Y. Tanaka and S. Kashiwaya, to be published in *Phys. Rev.* **B70** (2004), *cond-mat/0308123*.

111. H. Kashiwaya, A. Sawa, S. Kashiwaya, H. Yamasaki, M. Koyanagi, I. Kurosawa, Y. Tanaka, and I. Iguchi, *Physica* **C357-360**, 1610 (2001); H. Kashiwaya, I. Kurosawa, S. Kashiwaya, A. Sawa, and Y. Tanaka, *Phys. Rev.* **B68**, 054527 (2003).

112. Y. Asano, Y. Tanaka, and S. Kashiwaya, *Phys. Rev.* **B69**, 134501 (2004).

113. S. Kashiwaya, Y. Tanaka, M. Koyanagi, and K. Kajimura, *J. Phys. Chem.* **56**, 1721 (1995).

114. N. Kitaura, H. Itoh, Y. Asano, Y. Tanaka, J. Inoue, Y. Tanuma, and S. Kashiwaya, *J. Phys. Soc. Jpn.* **72**, 1718 (2003).

115. R.B. Laughlin, *Phys. Rev. Lett.* **80**, 5188 (1998).

116. G. Koren and N. Levy, *Europhys. Lett.* **59**, 121 (2002).

117. F. Tafuri and J.R. Kirtley, *Phys. Rev.* **B62**, 13934 (2000).

118. M. Aprili, E. Badica, and L.H. Greene, *Phys. Rev. Lett.* **83**, 4630 (1999).

119. R. Krupke and G. Deuscher, *Phys. Rev. Lett.* **83**, 4634 (1999).

120. A. Biswas, P. Fournier, M.M. Qazilbash, V.N. Smolyaninova, H. Balci, and R.L. Greene, *Phys. Rev. Lett.* **88**, 207004 (2002).

121. Y. Dagan and G. Deutscher, *Phys. Rev. Lett.* **87**, 177004 (2001).

122. L.H. Greene, P. Hentges, H. Aubin, M. Aprili, E. Badica, M. Covington, M.M. Pafford, G. Westwood, W.G. Klempere, S. Jian, and D.G. Hinks, *Physica* **C387**, 162 (2003).

123. A. Sawa, S. Kashiwaya, H. Obara, H. Yamasaki, M. Koyanagi, Y. Tanaka, and N. Yoshida, *Physica* **C339**, 107 (2000).

124. W.K. Neils and D.J. Van Harlingen, *Phys. Rev. Lett.* **88**, 047001 (2002).

125. Y. Asano and Y. Tanaka, *Phys. Rev.* **B65**, 064522 (2002).

126. Y. Asano, Y. Tanaka, and S. Kashiwaya, *cond-mat/0302287*.

127. Y. Asano and Y.Tanaka, *Toward the Controllable Quantum State*, H. Takayanagi and J. Nitta (eds.), World Scientific, Singapole (2003).

128. Y.S. Barash, A.A. Svidzinsky, and H. Burkhardt, *Phys. Rev.* **B55**, 15282 (1997).

129. Y. Tanaka, Y. Tanuma, and S. Kashiwaya, *Phys. Rev.* **B64**, 054510 (2001).

130. G. Eilenberger, *Z. Phys.* **214**, 195 (1968).

131. A.I. Larkin and Yu.N. Ovchinnikov, *Eksp. Teor. Fiz.* **55**, 2262 (1986) [*Sov. Phys. JETP* **28**, 1200 (1968).]

132. A.L. Schelankov, *J. Low. Temp. Phys.* **60**, 29 (1985).

133. P.A. Lee and D.S. Fisher, *Phys. Rev. Lett.* **47**, 882 (1981).

134. Y. Asano and G.E.W. Bauer, *Phys. Rev.* **B54**, 11602 (1996); *ibid*. **B54**, 9972 (1997).

135. H. Tsuchiura, Y. Tanaka, M. Ogata, and S. Kashiwaya, *Phys. Rev. Lett.* **84**, 3165 (2000).

136. M. Aprili, M. Covington, E. Paraoanu, B. Niedermeier, and L.H. Greene, *Phys. Rev.* **B57**, R8139 (1998).

137. Y. Asano, *Phys. Rev.* **B61**, 1732 (2000); Y. Asano and T. Kato, *J. Phys. Soc. Jpn.* **69**, 1125 (2000); Y. Asano and T. Yuito, *Phys. Rev.* **B62**, 7477 (2000).